DOI 10.2478/ama-2025-0005

DUAL THERMAL ANALYSIS OF FRACTIONAL CONVECTIVE FLOW THROUGH ALUMINUM OXIDE AND TITANIUM DIOXIDE NANOPARTICLES

Qasim ALI*, Rajai S. ALASSAR, Irfan. A. ABRO***, Kashif. A. ABRO******

*Faculty of Natural Sciences, Department of Mathematics, University of Chakwal, Chakwal 48800, Pakistan
**Faculty of Computing and Mathematics, Department of Mathematics, Interdisciplinary Research Center for Sustainable Energy Systems, King Fahd University of Petroleum & Minerals, Dhahran 31261, Saudi Arabia
***School of Materials Science and Engineering, Beijing Institute of Technology, Beijing 100081, China
****Faculty of Sciences, Technology and Humanities, Department of Basic Sciences and Related Studies, Mehran University of Engineering and Technology, Jamshoro, Pakistan

aliqasim829@gmail.com, rajaialassar@gmail.com, Irfan.abro@bit.edu.cn, kashif.abro@faculty.muet.edu.pk

received 05 January 2024, revised 04 March 2024, accepted 11 March 2024

Abstract: Dual assessing for thermal analysis via nanoparticles (aluminium oxide and titanium dioxide) and base fluids (water and blood) for mixed convection flows over an inclined plate is studied. The governing equations have been developed through fractional formats by exploiting modern definitions of CF (based on exponential function having no singularity) and AB (having non-singular and non-local kernel) fractional derivatives. This is an important theoretical and practical research that models the movement of heat in materials of various scales and heterogeneous media. The solution to the problem is achieved through Laplace transform with slip boundary and magnetic field. To explain the physical perception of fractional models, the dual fractional solutions of velocity field and temperature distribution are derived by comparing non-singularity and non-locality. The fractional solutions through numerical methods namely Stehfest and Tzou's have been invoked. The embedded thermo-dynamical fluctuating parameters have been traced out for the better performance of heat transfer. The results of temperature as well as velocity suggested decaying trends in characterization with rapid thermal analysis.

Keywords: Non-singularized derivative, Mixed convection flow with nanoparticles, Heat transfer of inclined plate, Integral transforms

1. INTRODUCTION

The applications of free convection flow are perceived in many fields of engineering and science such as heat exchangers, solar energy, drying processes, electric components of communication lines, and thermal storage systems. Several of its applications are also found in conservation, ventilation systems, dehydration, concentration, etc. These forms of flow are frequently inspected with a vertical plate in various manufacturing developments i.e., petroleum industry, geothermal phenomena, thermal insulation, etc. The free convection MHD flow with permeable plate by the AB derivatives along with integral transform is studied in [1]. In [2], free convection with NF in the presence of a magnetic field is deliberated by utilizing a fractional approach. A mathematical study with NFs with radiation impact is studied in [3]. A natural convection fluid flow with a long and vertical cylinder is considered in [4]. They studied the impacts of energy as well as mass transfer with time. Different investigators applied various techniques to study convection fluid flow with diverse structures [5-11].

Firstly, Choi presented NFs comprising nanoparticles in 1995. There are numerous uses of NFs in many fields for example fluid dynamics, in many engineering branches, and biomedical fields. NFs are considered the most excellent alternate ways to usual fluids [12-14]. The small particles in the base fluid which progress the competency of the characteristics of NFs for minimizing the system are known as nanoparticles and the key purpose of NFs is to realize the extreme possible heat conduction at a short nanoparticle concentration. The main conclusions have been distinguished because of the chemical configuration of the nanoparticles when are jumped in the base liquid i.e., reduced possibilities of erosion, thermal transmission, and solidity of the combination. These features play an exceptional part in increasing thermal transmission and energy proficiency in several fields i.e. biomedical instruments, microelectronics, and power generation [15]. Mud nanoparticles consume many practical uses in the penetrating of gasses and oil liquids because of their thermal conduction expressively. The growth of nanoparticles increases the thermal conduction and viscosity of NFs that oppose the intensifying temperature. Currently, because of their extensive uses in many branches of science and technology, NFs are now a fascinating and dominant field for research in fluid mechanics. The impacts of volume fraction and natural convection flow with NFs along with fractional calculus are studied in [16]. A viscous flow with NF (Titania-sodium cellulose) was discussed in [17]. To inspect and enhance the performance of solar accumulators exploited the NFs were studied by Farhana et al. [18]. Jamshed et al. [19-24] applied different techniques to study Eyring NF, Casson NF, second-grade NF, Williamson hybrid NF and tetra hybrid binary NF in different channels. Many researchers applied various methods to study NF flow models with diverse constructions [25-31].

In 1695 [32], firstly, the concept of fractional derivative was given by Leibnitz and L'Hospital which is a proficient tool related to memory facts. Memory function narrates to the kernel of the time-fractional derivative that has not simulated a physical development. Fractional calculus deals with non-local differentiation and integration [33]. The numerical solution of a fractional Oldroyd B-fluid is achieved by the modified Bessel equation as well as the Laplace method [34]. They showed that shear stress is improved as dynamic viscosity is increased. Fractional derivatives are most suitable to the problems of physical nature i.e., earth quick vibrations, polymers, viscoelasticity, heat transfer problems, fluid flows, etc. Over time, various algorithms and definitions were determined by different mathematicians. To find the solution to various mathematical models, the researchers used different fractional derivatives i.e., Riemann-Liouville, Caputo, CF, and AB derivatives. Fractional models can define more proficiently the consequences of the real nature of world problems such as electromagnetic theory, diffusive transfer, electrical networks, fluid flows, rheology, and viscoelastic materials. Then due to a few complications and limitations, Caputo and Fabrizio proposed the latest non-integer order model named CF fractional derivative along with an exponential and non-singular kernel [35-39].

According to the author's knowledge, there is no investigation on the study of mixed convection flow with Al_2O_3 and TiO_2 nanoparticles with water and blood-based NF in several situations which is a significant theoretical and practical study for the solution of important problems based on the fractional derivative. By getting motivation from these facts, our main purpose is to study a mixed convection flow with Al_2O_3 and TiO_2 nanoparticles with water and blood-based NF along with new definitions of fractional derivatives i.e., AB and CF fractional operators. A semi-analytical approach for AB and CF-based fractional models is applied by the Laplace transform technique along with Stehfest and Tzou's numerical schemes. To improve the novelty of the recent work some particular cases of velocity profile are also deliberated whose physical importance is prominent in the literature. The graphical illustration for the under-discussed mathematical problem by changing diverse flow parameters is underlined.

2. CHAPTER TITLE

We assume that a mixed convection fluid flow with Al_2O_3 and TiO_2 nanoparticles are flowing over an inclined plate with an inclination angle δ with the x-axis. Initially, when $t = 0$, the plate, as well as the fluid, is at rest and ambient medium temperature T_∞. When $t = 0^+$, the plate moves by a constant value of velocity $\frac{g(t)}{\mu}$ where $g(0) = 0$, and temperature increases from T_∞ to T_w. By this motion of the plate, the fluid begins to move over the plate. Along with all these conditions, it is also supposed the slip impacts the boundaries of the plate. A magnetic field with an angle, θ is also utilized upon the plate as revealed in Fig 1.

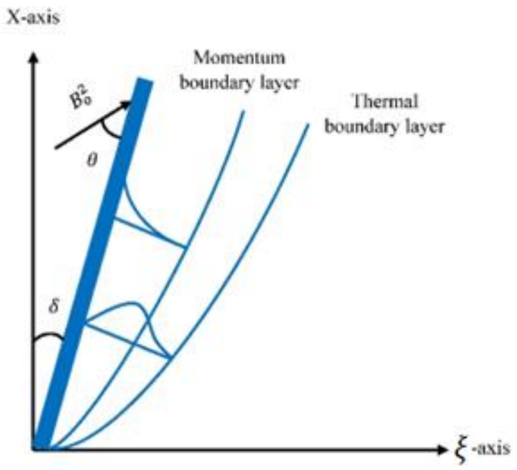

Fig 1. Geometry of the problem

We suppose the characteristics of the physical nanoparticles are from Table 1. The fluid velocity as well as the temperature depends on ξ and t. With Boussinesq's approximation and in the absence of pressure gradient [7, 45], the governing equations are:

Momentum Equation:

$$\rho_{nf}\frac{\partial w(\xi,t)}{\partial t} = \mu_{nf}\left(1+\alpha_1\frac{\partial}{\partial t}\right)\frac{\partial^2 w(\xi,t)}{\partial \xi^2} + g(\rho\beta_T)_{nf}[T(\xi,t)-T_\infty]Cos\delta - \sigma_{nf}B_o^2 Sin\theta\, w(\xi,t);\ \xi,t>0. \tag{1}$$

The thermal balance Equation:

$$\left(\rho C_p\right)_{nf}\frac{\partial T(\xi,t)}{\partial t} = -\frac{\partial q_1}{\partial \xi};\qquad \xi,t>0. \tag{2}$$

Fourier law [9]:

$$q_1(\xi,t) = -k_{nf}\frac{\partial T(\xi,t)}{\partial \xi} \tag{3}$$

with the appropriate initial and boundary conditions

$$w(\xi,0)=0,\qquad T(\xi,0)=T_\infty;\ \xi>0, \tag{4}$$

$$w(0,t) - b\left.\frac{\partial w(\xi,t)}{\partial \xi}\right|_{\xi=0} = \frac{g(t)}{\mu},\qquad T(0,t)=T_w;\ t>0 \tag{5}$$

$$w(\xi,t)\to 0,\qquad T(\xi,t)\to T_\infty;\qquad \xi\to\infty,\ t>0 \tag{6}$$

The appropriate non-dimensional parameters are taken as

$$\xi^* = \frac{\xi v_o}{v_f},\quad w^* = \frac{w}{U_o},\quad t^* = \frac{v_o^2 t}{v_f},\quad \vartheta^* = \frac{T-T_\infty}{T_w-T_\infty},$$

$$b^* = \frac{h}{k}b,\quad q^* = \frac{q}{q_o},\quad q_o = \frac{k_{nf}(T_w-T_\infty)v_o}{v_f},\ g^*(t^*) = \frac{1}{\mu}\sqrt{\frac{t_o}{v}}f(t_o t^*). \tag{7}$$

By using the above non-dimensional parameters in Eq. (7), the governing Eqs. (1)-(3) and equivalent conditions (4)-(6) take the form as

$$\frac{\partial w(\xi,t)}{\partial t} = \frac{1}{\Lambda_o\Lambda_1}\left(1+\beta_1\frac{\partial}{\partial t}\right)\frac{\partial^2 w(\xi,t)}{\partial \xi^2} + \frac{\Lambda_2}{\Lambda_o}Gr\,\vartheta(\xi,t)Cos\delta - \frac{1}{\Lambda_o}M\,Sin\theta\, w(\xi,t), \tag{8}$$

$$\Lambda_3 Pr\frac{\partial\vartheta(\xi,t)}{\partial t} = -\frac{\partial q(\xi,t)}{\partial \xi};\ \xi,t>0, \tag{9}$$

$$q(\xi,t) = -\Lambda_4\frac{\partial\vartheta(\xi,t)}{\partial \xi}, \tag{10}$$

along with corresponding conditions

$$w(\xi,0)=0,\qquad \vartheta(\xi,0)=0;\ \xi>0 \tag{11}$$

$$w(0,t) - b\left.\frac{\partial w(\xi,t)}{\partial \xi}\right|_{\xi=0} = g(t),\quad \vartheta(0,t)=1;\ t>0, \tag{12}$$

$$w(\xi,t)\to 0,\qquad \vartheta(\xi,t)\to 0;\ \xi\to\infty,\ t>0 \tag{13}$$

where:

$$\rho_{nf} = (1-\varphi)\rho_f + \varphi\rho_s,\ \mu_{nf} = \frac{\mu_f}{(1-\varphi)^{2.5}},$$

$$(\rho\beta)_{nf} = (1-\varphi)(\rho\beta)_f + \varphi(\rho\beta)_s,\quad \left(\rho C_p\right)_{nf} = (1-\varphi)\left(\rho C_p\right)_f + \varphi\left(\rho C_p\right)_s,$$

DOI 10.2478/ama-2025-0005

$$\frac{k_{nf}}{k_f}=\frac{k_s+2k_f-2\varphi(k_f-k_s)}{k_s+2k_f+2\varphi(k_f-k_s)},\quad \frac{\sigma_{nf}}{\sigma_f}=1+\left\{3\left(\frac{\sigma_s}{\sigma_f}-1\right)\varphi\right\}\left\{\left(\frac{\sigma_s}{\sigma_f}+2\right)-\left(\frac{\sigma_s}{\sigma_f}-1\right)\varphi\right\}^{-1},$$

$$\Lambda_o=(1-\varphi)+\varphi\frac{\rho_s}{\rho_f},\quad \Lambda_1=\frac{1}{(1-\varphi)^{2.5}},\quad \Lambda_2=(1-\varphi)+\varphi\frac{(\rho\beta_T)_s}{(\rho\beta_T)_f},$$

$$\Lambda_3=(1-\varphi)+\varphi\frac{(\rho C_p)_s}{(\rho C_p)_f},\quad \Lambda_4=\frac{k_{nf}}{k_f},\quad Pr=\frac{(\mu C_p)_f}{k_f},$$

$$Gr=\frac{g(\beta v)_f(T_w-T_\infty)}{U_o^3},\ M=\left(\frac{v_f}{v_o}\right)^2\frac{\sigma_{nf}B_0^2}{\rho_f v_f},\quad \beta_1=\alpha_1 v_f\left(\frac{v_f}{v_o}\right)^2.$$

Tab. 1. Thermophysical characteristics of base fluids (water and blood) and nanoparticles [6,38].

Material	H_2O	Blood	Al_2O_3	TiO_2
$\rho(kgm^{-3})$	997.1	1053	1600	4250
$C_p(kg^{-1}k^{-1})$	0.4179	3594	796	686.2
$K(Wm^{-1}k^{-1})$	0.613	0.492	3000	8.9528
$B_T\times 10^{-5}(k^{-1})$	21	0.18	44	0.90

2.1. Formulation of governing equations by using non-singular kernels

To formulate the fractional model recent proposed definitions of fractional derivatives i.e., AB and CF derivatives. The AB derivative of order 0$<\beta<1$ is defined as [41]

$$^{AB}\mathfrak{D}_t^\beta\ \mathrm{h}(t)=\frac{1}{\Gamma(1-\beta)}\int_0^t E_\beta\left(\frac{\beta(t-\varepsilon)^\beta}{(t-\varepsilon)}\right)h'(t)d\varepsilon;\ 0<\beta<1 \tag{14}$$

and $E_\beta(z)$ is a Mittage-Leffler function defined by

$$E_\beta(z)=\sum_{r=0}^{\infty}\frac{z^\beta}{\Gamma(r\beta+1)};\ 0<\ \beta<1,\ z\in\mathbb{C}.$$

The Laplace transform for the AB derivative is [42]

$$\mathcal{L}\left\{^{AB}\mathfrak{D}_t^\beta g(\xi,t)\right\}=\frac{q^\beta\mathcal{L}[g(\xi,t)]-q^{\beta-1}g(\xi,0)}{(1-\beta)q^\beta+\beta} \tag{15}$$

with

$$\lim_{\beta\to1}{}^{AB}\mathfrak{D}_t^\beta g(\xi,t)=\frac{\partial g(\xi,t)}{\partial t}.$$

The CF derivative of order 0$<\alpha<1$ is defined as [37,43]

$$^{CF}\mathfrak{D}_t^\alpha h(t)=\frac{1}{\Gamma(1-\alpha)}\int_0^t Exp\left(\frac{\beta(t-\varepsilon)^\beta}{(t-\varepsilon)}\right)h'(t)d\varepsilon,\ 0<\ \alpha<1, \tag{16}$$

The Laplace transform for the CF derivative is [27,38]

$$\mathcal{L}\{^{CF}\mathfrak{D}_t^\alpha g(\xi,t)\}=\frac{q\mathcal{L}[g(\xi,t)]-g(\xi,0)}{(1-\alpha)q+\alpha} \tag{17}$$

with

$$\lim_{\alpha\to1}{}^{CF}\mathfrak{D}_t^\alpha g(\xi,t)=\frac{\partial g(\xi,t)}{\partial t}.$$

It is important to note that AB and CF fractional operators can also be extended significantly by letting $\beta=1$ in Eq. (14) and $\alpha=1$ in Eq. (16) respectively.

The limitation of fractional parameters in derivatives, such as the AB and CF derivatives, to the interval $(0,1)$ derives from their interpretation and physical significance of these values. This range permits for a smooth transition across integer-order derivatives, recording abnormalities as well as long-memory effects in processes, making it ideal for modelling phenomena using sub-diffusive behaviour as well as memory-dependent dynamics in fields such as time series analysis, signal processing, and anomalous diffusion.

3. MODEL OF NANOFLUID WITH AB DERIVATIVE

The model to the problem with AB derivative can be expressed by substituting the ordinary derivative with AB derivative operator in Eqs. (8)-(10), we get

$$^{AB}\mathfrak{D}_t^\beta w(\xi,t)=\frac{1}{\Lambda_o\Lambda_1}\left(1+\beta_1{}^{AB}\mathfrak{D}_t^\beta\right)\frac{\partial^2 w(\xi,t)}{\partial\xi^2}+\frac{\Lambda_2}{\Lambda_o}Gr\ \vartheta(\xi,t)Cos\delta-\frac{1}{\Lambda_o}M\ Sin\theta\ w(\xi,t), \tag{18}$$

$$\Lambda_3 Pr^{AB}\mathfrak{D}_t^\beta\vartheta(\xi,t)=-\frac{\partial q(\xi,t)}{\partial\xi};\ \xi,t>0, \tag{19}$$

$$q(\xi,t)=-\Lambda_4\frac{\partial\vartheta(\xi,t)}{\partial\xi}. \tag{20}$$

3.1. Temperature with ab derivative

By employing the Laplace transform on Eqs. (19) and (20), we get

$$\frac{\partial^2\bar{\vartheta}(\xi,q)}{\partial\xi^2}-\frac{\Lambda_3 Pr}{\Lambda_4}\left(\frac{q^\beta}{(1-\beta)q^\beta+\beta}\right)\bar{\vartheta}(\xi,q)=0, \tag{21}$$

where $\bar{\vartheta}(\xi,q)$ is the Laplace transform for $\vartheta(\xi,t)$, and the transformed conditions after Laplace transform are as follows

$$\bar{\vartheta}(\xi,q)=\frac{1}{q}$$

and $\quad\bar{\vartheta}(\xi,q)\to0$ as $\xi\to\infty$. (22)

With the above conditions of Eq. (22), we get the temperature as

$$\bar{\vartheta}(\xi,q)=\frac{1}{q}e^{-\xi\sqrt{\frac{\Lambda_3 Pr}{\Lambda_4}\left(\frac{q^\beta}{(1-\beta)q^\beta+\beta}\right)}}. \tag{23}$$

Eq (23) can be written as

$$\bar{\vartheta}(\xi,q)=\frac{1}{q}e^{-\xi\sqrt{\frac{c_1 q^{\gamma}}{q^{\gamma}+c_2}}} \tag{24}$$

where:

$$c_1=\frac{\Lambda_3 Pr\,\gamma}{\Lambda_4},\qquad c_2=\beta\gamma,\qquad \gamma=\frac{1}{1-\beta}.$$

Eq (24) can also be written in summation form as

$$\bar{\vartheta}(\xi,q)=\frac{1}{q}+\sum_{a_1=1}^{\infty}\sum_{a_2=0}^{\infty}\frac{(-\xi\sqrt{c_1})^{a_1}}{a_1!}\frac{(-c_2)^{a_2}}{q^{1+a_2\beta}}\frac{\Gamma\left(\frac{a_1}{2}+a_2\right)}{\Gamma\left(\frac{a_1}{2}\right)\Gamma(a_2+1)} \tag{25}$$

By taking the Laplace inverse of Eq. (25), we have

$$\vartheta(\xi,t)=1+\sum_{a_1=1}^{\infty}\sum_{a_2=0}^{\infty}\frac{(-\xi\sqrt{c_1})^{a_1}}{a_1!}\frac{\Gamma\left(\frac{a_1}{2}+a_2\right)}{\Gamma\left(\frac{a_1}{2}\right)\Gamma(a_2+1)}\frac{(-c_2)^{a_2}\,t^{a_2\beta}}{\Gamma(1+a_2\beta)} \tag{26}$$

When $\beta\to 1$, Eq. (26) becomes

$$\vartheta(\xi,t)=\frac{\xi\left(1-erf\left(\frac{|\xi|\sqrt{\Lambda_3 Pr}}{2\sqrt{\Lambda_4 t}}\right)\right)}{|\xi|};\qquad \xi,\sqrt{\frac{\Lambda_3 Pr}{\Lambda_4}}>0. \tag{27}$$

3.2. Velocity with ab derivative

By using the Laplace transform on Eq. (18), we get

$$\left(\frac{q^{\beta}}{(1-\beta)q^{\beta}+\beta}\right)\bar{w}(\xi,q)=\frac{1}{\Lambda_o\Lambda_1}\left(1+\beta_1\frac{q^{\beta}}{(1-\beta)q^{\beta}+\beta}\right)\frac{\partial^2\bar{w}(\xi,q)}{\partial\xi^2}+\frac{\Lambda_2}{\Lambda_o}Gr\,Cos\delta\,\bar{\vartheta}(\xi,q)-\frac{1}{\Lambda_o}M\,Sin\theta\,\bar{w}(\xi,q) \tag{28}$$

with the corresponding conditions

$$\bar{w}(0,q)-b\left.\frac{\partial\bar{w}(\xi,q)}{\partial\xi}\right|_{\xi=0}=G(q)$$

and

$$\bar{w}(\xi,q)\to 0\quad as\quad \xi\to\infty. \tag{29}$$

Eq (28) is solved by utilizing Eq. (29) and we get

$$\bar{w}(\xi,q)=\frac{1}{1+b\sqrt{\frac{\Lambda_o\Lambda_1\gamma q^{\beta}+\left(q^{\beta}+\beta\gamma\right)\Lambda_1 M Sin\theta}{q^{\beta}+\beta\gamma+\beta_1 q^{\beta}\gamma}}}\left(\frac{\Lambda_2 Gr\,Cos\delta}{\Lambda_o q}\frac{1}{\frac{\Lambda_3 Pr}{\Lambda_4}\left(\frac{q^{\beta}\gamma}{q^{\beta}+\beta\gamma}\right)-\frac{\Lambda_o\Lambda_1\gamma q^{\beta}+\left(q^{\beta}+\beta\gamma\right)\Lambda_1 M\,Sin\theta}{q^{\beta}+\beta\gamma+\beta_1 q^{\beta}\gamma}}\left(1+b\sqrt{\frac{\Lambda_3 Pr}{\Lambda_4}\left(\frac{q^{\beta}\gamma}{q^{\beta}+\beta\gamma}\right)}\right)+G(q)\right)e^{-\xi\sqrt{\frac{\Lambda_o\Lambda_1\gamma q^{\beta}+\left(q^{\beta}+\beta\gamma\right)\Lambda_1 M\,Sin\theta}{q^{\beta}+\beta\gamma+\beta_1 q^{\beta}\gamma}}}-\frac{\Lambda_2 Gr\,Cos\delta}{\Lambda_o q}\frac{1}{\frac{\Lambda_3 Pr}{\Lambda_4}\left(\frac{q^{\beta}\gamma}{q^{\beta}+\beta\gamma}\right)-\frac{\Lambda_o\Lambda_1\gamma q^{\beta}+\left(q^{\beta}+\beta\gamma\right)\Lambda_1 M\,Sin\theta}{q^{\beta}+\beta\gamma+\beta_1 q^{\beta}\gamma}}e^{-\xi\sqrt{\frac{\Lambda_3 Pr}{\Lambda_4}\left(\frac{q^{\beta}\gamma}{q^{\beta}+\beta\gamma}\right)}}. \tag{30}$$

When $\beta\to 1$, Eq. (30) becomes

$$\bar{w}(\xi,q)=\frac{1}{1+b\sqrt{\frac{\Lambda_o\Lambda_1 q+\Lambda_1 M\,Sin\theta}{1+\beta_1 q}}}\left(\frac{\Lambda_2 Gr\,Cos\delta}{\Lambda_o q}\frac{1}{\frac{\Lambda_3 Pr}{\Lambda_4}q-\frac{\Lambda_o\Lambda_1 q+\Lambda_1 M\,Sin\theta}{1+\beta_1 q}}\left(1+b\sqrt{\frac{\Lambda_3 Pr}{\Lambda_4}q}\right)+G(q)\right)e^{-\xi\sqrt{\frac{\Lambda_o\Lambda_1 q+\Lambda_1 M\,Sin\theta}{1+\beta_1 q}}}-\frac{\Lambda_2 Gr\,Cos\delta}{\Lambda_o q}\frac{1}{\frac{\Lambda_3 Pr}{\Lambda_4}q-\frac{\Lambda_o\Lambda_1 q+\Lambda_1 M\,Sin\theta}{1+\beta_1 q}}e^{-\xi\sqrt{\frac{\Lambda_3 Pr}{\Lambda_4}q}} \tag{31}$$

The Laplace inverse of these solutions is determined numerically through Stehfest as well as Tzou's approaches as in Tables 2-3.

4. MODEL OF NANOFLUID WITH CF DERIVATIVE

In the above section, the temperature, as well as velocity, is determined by using the AB-fractional derivative, now the modelling of governing equations by CF-fractional derivative may be expressed by replacing the ordinary derivative with CF-fractional derivative operative ${}^{CF}\mathfrak{D}_t^{\alpha}$, the governing equations for the CF-fractional derivative model are attained as

$${}^{CF}\mathfrak{D}_t^{\alpha}w(\xi,t)=\frac{1}{\Lambda_o\Lambda_1}\left(1+\beta_1\,{}^{CF}\mathfrak{D}_t^{\alpha}\right)\frac{\partial^2 w(\xi,t)}{\partial\xi^2}+\frac{\Lambda_2}{\Lambda_o}Gr\,\vartheta(\xi,t)Cos\delta-\frac{1}{\Lambda_o}M\,Sin\theta\,w(\xi,t), \tag{32}$$

$$\Lambda_3 Pr\,{}^{CF}\mathfrak{D}_t^{\alpha}\vartheta(\xi,t)=-\frac{\partial q(\xi,t)}{\partial\xi};\qquad \xi,t>0, \tag{33}$$

$$q(\xi,t)=-\Lambda_4\frac{\partial\vartheta(\xi,t)}{\partial\xi}. \tag{34}$$

4.1. Temperature with cf derivative

By taking Laplace transform on Eqs. (33), and (34), we get

$$\frac{\partial^2\bar{\vartheta}(\xi,q)}{\partial\xi^2}-\frac{\Lambda_3 Pr}{\Lambda_4}\left(\frac{q}{(1-\alpha)q+\alpha}\right)\bar{\vartheta}(\xi,q)=0. \tag{35}$$

By using the corresponding conditions of Eq. (22), the solution of Eq. (35) is

$$\bar{\vartheta}(\xi,q)=\frac{1}{q}e^{-\xi\sqrt{\frac{\Lambda_3 Pr}{\Lambda_4}\left(\frac{q}{(1-\alpha)q+\alpha}\right)}}. \tag{36}$$

Eq (36) can be written as

$$\bar{\vartheta}(\xi,q)=\frac{1}{q}e^{-\xi\sqrt{\frac{d_1 q}{q+d_2}}} \tag{37}$$

DOI 10.2478/ama-2025-0005

Where

$$d_1 = \frac{\Lambda_3 Pr\,\gamma}{\Lambda_4}, \qquad d_2 = \alpha\gamma, \qquad \gamma = \frac{1}{1-\alpha}$$

Eq (37) may be written in summation form as

$$\bar{\vartheta}(\xi,q) = \frac{1}{q} + \sum_{a_1=1}^{\infty}\sum_{a_2=0}^{\infty}\frac{\left(-\xi\sqrt{d_1}\right)^{a_1}}{a_1!}\frac{(-d_2)^{a_2}}{q^{1+a_2}}\frac{\Gamma\left(\frac{a_1}{2}+a_2\right)}{\Gamma\left(\frac{a_1}{2}\right)\Gamma(a_2+1)} \quad (38)$$

By utilizing the Laplace inverse of Eq. (38), we have

$$\vartheta(\xi,t) = 1 + \sum_{a_1=1}^{\infty}\sum_{a_2=0}^{\infty}\frac{\left(-\xi\sqrt{d_1}\right)^{a_1}}{a_1!}\frac{(-d_2)^{a_2}\,t^{a_2}}{\Gamma(a_2+1)}\frac{\Gamma\left(\frac{a_1}{2}+a_2\right)}{\Gamma\left(\frac{a_1}{2}\right)\Gamma(a_2+1)} \quad (39)$$

For the special case for ordinary solution replace $\alpha \to 1$ in Eq (39), and then the solution will be

$$\vartheta(\xi,t) = \frac{\xi\left(1-erf\left(\frac{|\xi|\sqrt{\Lambda_3 Pr}}{2\sqrt{\Lambda_4 t}}\right)\right)}{|\xi|}\ ;\ \xi,\ \sqrt{\frac{\Lambda_3 Pr}{\Lambda_4}} > 0. \quad (40)$$

4.2. Velocity with cf derivative

By using the Laplace transform on Eqs. (32), we get

$$\left(\frac{s}{(1-\alpha)s+\alpha}\right)\bar{w}(\xi,s) = \frac{1}{\Lambda_o\Lambda_1}\left(1+\beta_1\left(\frac{s}{(1-\alpha)s+\alpha}\right)\right)\frac{\partial^2\bar{w}(\xi,s)}{\partial\xi^2} + \frac{\Lambda_2}{\Lambda_o}Gr\,\bar{\vartheta}(\xi,s)Cos\delta - \frac{1}{\Lambda_o}M\,Sin\theta\bar{w}(\xi,s). \quad (41)$$

By solving Eq (41) with the corresponding conditions in Eq. (29), we get

$$\bar{w}(\xi,q) = \frac{1}{1+b\sqrt{\frac{\Lambda_o\Lambda_1\gamma q+(q+\alpha\gamma)\Lambda_1 M\,Sin\theta}{q+\alpha\gamma+\beta_1 q\gamma}}}\left(\frac{\Lambda_2 Gr\ Cos\delta}{\Lambda_o s}\frac{1}{\frac{\Lambda_3 Pr}{\Lambda_4}\left(\frac{q\gamma}{q+\alpha\gamma}\right)-\frac{\Lambda_o\Lambda_1\gamma q+(q+\alpha\gamma)\Lambda_1 M\,Sin\theta}{q+\alpha\gamma+\beta_1 q\gamma}}\left(1+b\sqrt{\frac{\Lambda_3 Pr}{\Lambda_4}\left(\frac{q\gamma}{q+\alpha\gamma}\right)}\right)+G(q)\right)e^{-\xi\sqrt{\frac{\Lambda_o\Lambda_1\gamma q+(q+\alpha\gamma)\Lambda_1 M\,Sin\theta}{q+\alpha\gamma+\beta_1 q\gamma}}}$$
$$-\frac{\Lambda_2 Gr\ Cos\delta}{\Lambda_o q}\frac{1}{\frac{\Lambda_3 Pr}{\Lambda_4}\left(\frac{q\gamma}{q+\alpha\gamma}\right)-\frac{\Lambda_o\Lambda_1\gamma q+(q+\alpha\gamma)\Lambda_1 M\,Sin\theta}{q+\alpha\gamma+\beta_1 q\gamma}}e^{-\xi\sqrt{\frac{\Lambda_3 Pr}{\Lambda_4}\left(\frac{q\gamma}{q+\alpha\gamma}\right)}}. \quad (42)$$

When $\alpha \to 1$, Eq. (42) becomes

$$\bar{w}(\xi,q) = \frac{1}{1+b\sqrt{\frac{\Lambda_o\Lambda_1 q+\Lambda_1 M\,Sin\theta}{1+\beta_1 q}}}\left(\frac{\Lambda_2 Gr\ Cos\delta}{\Lambda_o q}\frac{1}{\frac{\Lambda_3 Pr}{\Lambda_4}q-\frac{\Lambda_o\Lambda_1 q+\Lambda_1 M\,Sin\theta}{1+\beta_1 q}}\left(1+b\sqrt{\frac{\Lambda_3 Pr}{\Lambda_4}q}\right)+G(q)\right)e^{-\xi\sqrt{\frac{\Lambda_o\Lambda_1 q+\Lambda_1 M\,Sin\theta}{1+\beta_1 q}}} -$$
$$\frac{\Lambda_2 Gr\ Cos\delta}{\Lambda_o q}\frac{1}{\frac{\Lambda_3 Pr}{\Lambda_4}q-\frac{\Lambda_o\Lambda_1 q+\Lambda_1 M\,Sin\theta}{1+\beta_1 q}}e^{-\xi\sqrt{\frac{\Lambda_3 Pr}{\Lambda_4}q}}. \quad (43)$$

To find out the Laplace inverse, various researchers applied different numerical approaches to find the solution of diverse differential fractional models as in [44-47]. Consequently, here we will also utilize the Stehfest scheme to find the numerical solution of temperature as well as velocity numerically. Grave Stehfest scheme [48] can be expressed as

$$w(\xi,t) = \frac{ln(2)}{t}\sum_{n=1}^{M}v_n\,\bar{w}\left(\xi, n\frac{ln(2)}{t}\right) \quad (44)$$

where M be a non-negative integer, and

$$v_n = (-1)^{n+\frac{M}{2}}\sum_{p=\left[\frac{q+1}{2}\right]}^{min\left(q,\frac{M}{2}\right)}\frac{p^{\frac{M}{2}}\,(2p)!}{\left(\frac{M}{2}-p\right)!p!\,(p-1)!\,(q-p)!\,(2p-q)!} \quad (45)$$

However, we also applied another estimation for temperature as well as velocity solutions, Tzou's method for the comparison and validation of our numerical findings with the Stehfest [48] scheme. Tzou's scheme [49] has the form as

$$w(\xi,t) = \frac{e^{4.7}}{t}\left[\frac{1}{2}\bar{w}\left(r,\frac{4.7}{t}\right) + Re\left\{\sum_{j=1}^{N}(-1)^k\,\bar{w}\left(r,\frac{4.7+k\pi i}{t}\right)\right\}\right] \quad (46)$$

where i and $Re(.)$ are imaginary units and real portions and $N > 1$ is a natural number.

5. PARTICULAR CASES

As the solution of the velocity field with AB and CF derivative in Eq. (30) and (42) correspondingly, is in a more general form. Consequently, to demonstrate some more physical perception of the problem, we will deliberate some particular cases for the function $g(t)$ for the velocity whose physical explanation is prominent in the literature.

Case 1: $\boldsymbol{g(t) = t}$

In this case, we take $g(t) = t$ then the expressions of velocity with AB and CF derivative along with Eqs. (30) and (42) respectively will take the form as

$$\bar{w}(\xi,q) = \frac{1}{1+b\sqrt{\frac{\Lambda_o\Lambda_1\gamma q^\beta+\left(q^\beta+\beta\gamma\right)\Lambda_1 M\ Sin\theta}{q^\beta+\beta\gamma+\beta_1 q^\beta\gamma}}},$$
$$\left(\frac{\Lambda_2 Gr\ Cos\delta}{\Lambda_o q}\frac{1}{\frac{\Lambda_3 Pr}{\Lambda_4}\left(\frac{q^\beta\gamma}{q^\beta+\beta\gamma}\right)-\frac{\Lambda_o\Lambda_1\gamma q^\beta+\left(q^\beta+\beta\gamma\right)\Lambda_1 M\ Sin\theta}{q^\beta+\beta\gamma+\beta_1 q^\beta\gamma}}\left(1+b\sqrt{\frac{\Lambda_3 Pr}{\Lambda_4}\left(\frac{q^\beta\gamma}{q^\beta+\beta\gamma}\right)}\right)+\frac{1}{q^2}\right)e^{-\xi\sqrt{\frac{\Lambda_o\Lambda_1\gamma q^\beta+\left(q^\beta+\beta\gamma\right)\Lambda_1 M\ Sin\theta}{q^\beta+\beta\gamma+\beta_1 q^\beta\gamma}}}$$
$$-\frac{\Lambda_2 Gr\ Cos\delta}{\Lambda_o q}\frac{1}{\frac{\Lambda_3 Pr}{\Lambda_4}\left(\frac{q^\beta\gamma}{q^\beta+\beta\gamma}\right)-\frac{\Lambda_o\Lambda_1\gamma q^\beta+\left(q^\beta+\beta\gamma\right)\Lambda_1 M\ Sin\theta}{q^\beta+\beta\gamma+\beta_1 q^\beta\gamma}}e^{-\xi\sqrt{\frac{\Lambda_3 Pr}{\Lambda_4}\left(\frac{q^\beta\gamma}{q^\beta+\beta\gamma}\right)}} \quad (47)$$

DOI 10.2478/ama-2025-0005 acta mechanica et automatica, vol.19 no.1 (2025)

and
$$\bar{w}(\xi,q)=\frac{1}{1+b\sqrt{\frac{\Lambda_o\Lambda_1\gamma q+(q+\alpha\gamma)\Lambda_1 M\ Sin\theta}{q+\alpha\gamma+\beta_1 q\gamma}}}\left(\frac{\Lambda_2 Gr\ Cos\delta}{\Lambda_o q}\ \frac{1}{\frac{\Lambda_3 Pr}{\Lambda_4}\left(\frac{q\gamma}{q+\alpha\gamma}\right)-\frac{\Lambda_o\Lambda_1\gamma q+(q+\alpha\gamma)\Lambda_1 M\ Sin\theta}{q+\alpha\gamma+\beta_1 q\gamma}}\left(1+b\sqrt{\frac{\Lambda_3 Pr}{\Lambda_4}\left(\frac{q\gamma}{q+\alpha\gamma}\right)}\right)+\frac{1}{q^2}\right)e^{-\xi\sqrt{\frac{\Lambda_o\Lambda_1\gamma q+(q+\alpha\gamma)\Lambda_1 M\ Sin\theta}{q+\alpha\gamma+\beta_1 q\gamma}}}$$
$$-\frac{\Lambda_2 Gr\ Cos\delta}{\Lambda_o s}\ \frac{1}{\frac{\Lambda_3 Pr}{\Lambda_4}\left(\frac{q\gamma}{q+\alpha\gamma}\right)-\frac{\Lambda_o\Lambda_1\gamma q+(q+\alpha\gamma)\Lambda_1 M\ Sin\theta}{q+\alpha\gamma+\beta_1 q\gamma}}\ e^{-\xi\sqrt{\frac{\Lambda_3 Pr}{\Lambda_4}\left(\frac{q\gamma}{q+\alpha\gamma}\right)}}. \quad (48)$$

Case 2: $\boldsymbol{g(t)=Sin(\omega t)}$

In this case, we take $g(t)=Sin(\omega t)$ where ω denotes the intensity of the shear stress, then the expressions for velocity with AB and CF derivative with Eqs. (30) and (42) correspondingly will take the form as

$$\bar{w}(\xi,q)=\frac{1}{1+b\sqrt{\frac{\Lambda_o\Lambda_1\gamma q^\beta+\left(q^\beta+\beta\gamma\right)\Lambda_1 M\ Sin\theta}{q^\beta+\beta\gamma+\beta_1 q^\beta\gamma}}}\left(\frac{\Lambda_2 Gr\ Cos\delta}{\Lambda_o q}\ \frac{1}{\frac{\Lambda_3 Pr}{\Lambda_4}\left(\frac{q^\beta\gamma}{q^\beta+\beta\gamma}\right)-\frac{\Lambda_o\Lambda_1\gamma q^\beta+\left(q^\beta+\beta\gamma\right)\Lambda_1 M\ Sin\theta}{q^\beta+\beta\gamma+\beta_1 q^\beta\gamma}}\left(1+b\sqrt{\frac{\Lambda_3 Pr}{\Lambda_4}\left(\frac{q^\beta\gamma}{q^\beta+\beta\gamma}\right)}\right)+\frac{\omega}{\omega^2+q^2}\right)e^{-\xi\sqrt{\frac{\Lambda_o\Lambda_1\gamma q^\beta+\left(q^\beta+\beta\gamma\right)\Lambda_1 M\ Sin\theta}{q^\beta+\beta\gamma+\beta_1 q^\beta\gamma}}}$$
$$-\frac{\Lambda_2 Gr\ Cos\delta}{\Lambda_o q}\ \frac{1}{\frac{\Lambda_3 Pr}{\Lambda_4}\left(\frac{q^\beta\gamma}{q^\beta+\beta\gamma}\right)-\frac{\Lambda_o\Lambda_1\gamma q^\beta+\left(q^\beta+\beta\gamma\right)\Lambda_1 M\ Sin\theta}{q^\beta+\beta\gamma+\beta_1 q^\beta\gamma}}\ e^{-\xi\sqrt{\frac{\Lambda_3 Pr}{\Lambda_4}\left(\frac{q^\beta\gamma}{q^\beta+\beta\gamma}\right)}} \quad (49)$$

and

$$\bar{w}(\xi,q)=\frac{1}{1+b\sqrt{\frac{\Lambda_o\Lambda_1\gamma q+(q+\alpha\gamma)\Lambda_1 M\ Sin\theta}{q+\alpha\gamma+\beta_1 q\gamma}}}\left(\frac{\Lambda_2 Gr\ Cos\delta}{\Lambda_o q}\ \frac{1}{\frac{\Lambda_3 Pr}{\Lambda_4}\left(\frac{q\gamma}{q+\alpha\gamma}\right)-\frac{\Lambda_o\Lambda_1\gamma q+(q+\alpha\gamma)\Lambda_1 M\ Sin\theta}{q+\alpha\gamma+\beta_1 q\gamma}}\left(1+b\sqrt{\frac{\Lambda_3 Pr}{\Lambda_4}\left(\frac{q\gamma}{q+\alpha\gamma}\right)}\right)+\frac{\omega}{\omega^2+q^2}\right)e^{-\xi\sqrt{\frac{\Lambda_o\Lambda_1\gamma q+(q+\alpha\gamma)\Lambda_1 M\ Sin\theta}{q+\alpha\gamma+\beta_1 q\gamma}}}$$
$$-\frac{\Lambda_2 G\ Cos\delta}{\Lambda_o q}\ \frac{1}{\frac{\Lambda_3 Pr}{\Lambda_4}\left(\frac{q\gamma}{q+\alpha\gamma}\right)-\frac{\Lambda_o\Lambda_1\gamma q+(q+\alpha\gamma)\Lambda_1 M\ Sin\theta}{q+\alpha\gamma+\beta_1 q\gamma}}\ e^{-\xi\sqrt{\frac{\Lambda_3 Pr}{\Lambda_4}\left(\frac{q\gamma}{q+\alpha\gamma}\right)}} \quad (50)$$

Case 3: $\boldsymbol{g(t)=t\ Cos(t)}$

In this case, we take $g(t)=t\ Cost$ with its Laplace $G(q)=\frac{q^2-1}{(q^2+1)^2}$, then the expressions of velocity through AB and CF derivative along with Eqs. (30) and (42) correspondingly will take the form as

$$\bar{w}(\xi,q)=\frac{1}{1+b\sqrt{\frac{\Lambda_o\Lambda_1\gamma q^\beta+\left(q^\beta+\beta\gamma\right)\Lambda_1 M\ Sin\theta}{q^\beta+\beta\gamma+\beta_1 q^\beta\gamma}}}\left(\frac{\Lambda_2 Gr\ Cos\delta}{\Lambda_o q}\ \frac{1}{\frac{\Lambda_3 Pr}{\Lambda_4}\left(\frac{q^\beta\gamma}{q^\beta+\beta\gamma}\right)-\frac{\Lambda_o\Lambda_1\gamma q^\beta+\left(q^\beta+\beta\gamma\right)\Lambda_1 M\ Sin\theta}{q^\beta+\beta\gamma+\beta_1 q^\beta\gamma}}\left(1+b\sqrt{\frac{\Lambda_3 Pr}{\Lambda_4}\left(\frac{q^\beta\gamma}{q^\beta+\beta\gamma}\right)}\right)+\frac{q^2-1}{(1+q^2)^2}\right)e^{-\xi\sqrt{\frac{\Lambda_o\Lambda_1\gamma q^\beta+\left(q^\beta+\beta\gamma\right)\Lambda_1 M\ Sin\theta}{q^\beta+\beta\gamma+\beta_1 q^\beta\gamma}}}$$
$$-\frac{\Lambda_2 Gr\ Cos\delta}{\Lambda_o q}\ \frac{1}{\frac{\Lambda_3 Pr}{\Lambda_4}\left(\frac{q^\beta\gamma}{q^\beta+\beta\gamma}\right)-\frac{\Lambda_o\Lambda_1\gamma q^\beta+\left(q^\beta+\beta\gamma\right)\Lambda_1 M\ Sin\theta}{q^\beta+\beta\gamma+\beta_1 q^\beta\gamma}}\ e^{-\xi\sqrt{\frac{\Lambda_3 Pr}{\Lambda_4}\left(\frac{q^\beta\gamma}{q^\beta+\beta\gamma}\right)}} \quad (51)$$

and

$$\bar{w}(\xi,q)=\frac{1}{1+b\sqrt{\frac{\Lambda_o\Lambda_1\gamma q+(q+\alpha\gamma)\Lambda_1 M\ Sin\theta}{q+\alpha\gamma+\beta_1 q\gamma}}}\left(\frac{\Lambda_2 Gr\ Cos\delta}{\Lambda_o q}\ \frac{1}{\frac{\Lambda_3 Pr}{\Lambda_4}\left(\frac{q\gamma}{q+\alpha\gamma}\right)-\frac{\Lambda_o\Lambda_1\gamma q+(q+\alpha\gamma)\Lambda_1 M\ Sin\theta}{q+\alpha\gamma+\beta_1 q\gamma}}\left(1+b\sqrt{\frac{\Lambda_3 Pr}{\Lambda_4}\left(\frac{q\gamma}{q+\alpha\gamma}\right)}\right)+\frac{q^2-1}{(1+q^2)^2}\right)e^{-\xi\sqrt{\frac{\Lambda_o\Lambda_1\gamma q+(q+\alpha\gamma)\Lambda_1 M\ Sin\theta}{q+\alpha\gamma+\beta_1 q\gamma}}}$$
$$-\frac{\Lambda_2 Gr\ Cos\delta}{\Lambda_o q}\ \frac{1}{\frac{\Lambda_3 Pr}{\Lambda_4}\left(\frac{q\gamma}{q+\alpha\gamma}\right)-\frac{\Lambda_o\Lambda_1\gamma q+(q+\alpha\gamma)\Lambda_1 M\ Sin\theta}{q+\alpha\gamma+\beta_1 q\gamma}}\ e^{-\xi\sqrt{\frac{\Lambda_3 Pr}{\Lambda_4}\left(\frac{q\gamma}{q+\alpha\gamma}\right)}}. \quad (52)$$

Case 4: $\boldsymbol{g(t)=t\ e^t}$

In the final case, we take $g(t)=te^t$ with its Laplace $G(q)=\frac{1}{(q-1)^2}$, then the expressions of velocity through AB and CF derivative along with Eqs. (30), and (42) correspondingly will take the form as

$$\bar{w}(\xi,q)=\frac{1}{1+b\sqrt{\frac{\Lambda_o\Lambda_1\gamma q^\beta+\left(q^\beta+\beta\gamma\right)\Lambda_1 M\ Sin\theta}{q^\beta+\beta\gamma+\beta_1 q^\beta\gamma}}}\left(\frac{\Lambda_2 Gr\ Cos\delta}{\Lambda_o q}\ \frac{1}{\frac{\Lambda_3 Pr}{\Lambda_4}\left(\frac{q^\beta\gamma}{q^\beta+\beta\gamma}\right)-\frac{\Lambda_o\Lambda_1\gamma q^\beta+\left(q^\beta+\beta\gamma\right)\Lambda_1 M\ Sin\theta}{q^\beta+\beta\gamma+\beta_1 q^\beta\gamma}}\left(1+b\sqrt{\frac{\Lambda_3 Pr}{\Lambda_4}\left(\frac{q^\beta\gamma}{q^\beta+\beta\gamma}\right)}\right)+\frac{1}{(q-1)^2}\right)e^{-\xi\sqrt{\frac{\Lambda_o\Lambda_1\gamma q^\beta+\left(q^\beta+\beta\gamma\right)\Lambda_1 M\ Sin\theta}{q^\beta+\beta\gamma+\beta_1 q^\beta\gamma}}}$$
$$-\frac{\Lambda_2 Gr\ Cos\delta}{\Lambda_o q}\ \frac{1}{\frac{\Lambda_3 Pr}{\Lambda_4}\left(\frac{q^\beta\gamma}{q^\beta+\beta\gamma}\right)-\frac{\Lambda_o\Lambda_1\gamma q^\beta+\left(q^\beta+\beta\gamma\right)\Lambda_1 M\ Sin\theta}{q^\beta+\beta\gamma+\beta_1 q^\beta\gamma}}\ e^{-\xi\sqrt{\frac{\Lambda_3 Pr}{\Lambda_4}\left(\frac{q^\beta\gamma}{q^\beta+\beta\gamma}\right)}} \quad (53)$$

DOI 10.2478/ama-2025-0005

and $\overline{w}(\xi,q)=\frac{1}{1+b\sqrt{\frac{\Lambda_o\Lambda_1\gamma q+(q+\alpha\gamma)\Lambda_1 M\ Sin\theta}{q+\alpha\gamma+\beta_1 q\gamma}}}$

$$\left(\frac{\Lambda_2 Gr\ Cos\delta}{\Lambda_o q}\ \frac{1}{\frac{\Lambda_3 Pr}{\Lambda_4}\left(\frac{q\gamma}{q+\alpha\gamma}\right)-\frac{\Lambda_o\Lambda_1\gamma q+(q+\alpha\gamma)\Lambda_1 M\ Sin\theta}{q+\alpha\gamma+\beta_1 q\gamma}}\left(1+b\sqrt{\frac{\Lambda_3 Pr}{\Lambda_4}\left(\frac{q\gamma}{q+\alpha\gamma}\right)}\right)+\frac{1}{(q-1)^2}\right)e^{-\xi\sqrt{\frac{\Lambda_o\Lambda_1\gamma q+(q+\alpha\gamma)\Lambda_1 M\ Sin\theta}{q+\alpha\gamma+\beta_1 q\gamma}}}$$

$$-\frac{\Lambda_2 Gr\ Cos\delta}{\Lambda_o q}\ \frac{1}{\frac{\Lambda_3 Pr}{\Lambda_4}\left(\frac{q\gamma}{q+\alpha\gamma}\right)-\frac{\Lambda_o\Lambda_1\gamma q+(q+\alpha\gamma)\Lambda_1 M\ Sin\theta}{q+\alpha\gamma+\beta_1 q\gamma}}\ e^{-\xi\sqrt{\frac{\Lambda_3 Pr}{\Lambda_4}\left(\frac{q\gamma}{q+\alpha\gamma}\right)}}. \tag{54}$$

6. RESULTS AND DISCUSSION

The mixed convection fluid flow with Al_2O_3 and TiO_2 nanoparticles with water and blood as base fluids are investigated with a slip effect at the boundaries on an inclined plane under the magnetic field by using AB and CF derivative schemes. The solution for the considered problem is explored with the Laplace scheme and numerical approaches i.e., Stehfest and Tzou for the inversion phenomenon of the Laplace transform. To obtain some physical features of velocity attained with AB and CF derivatives, some particular cases are also discussed. For studying the impacts of diverse flow parameters i.e., fractional parameters (α,β), angle of inclination, magnetic parameter, volume fraction, $Pr,$ and Grashof number, graphical diagrams are presented in Figs 2-9 through Mathematica.

The impact of fractional parameters (α,β), on temperature is shown in Figs. 2(a, b). By raising the estimations of α,β, the temperature illustrates decaying behaviour (at a small time) and an increasing trend at a large time, consequently, we see that the fractional parameters have dual behaviour (for small and large time) for temperature. This specifies the consequence of the CF and AB fractional operators that promise to illustrate the generalized memory and hereditary features. This is due to the different properties of CF (based on exponential function having no singularity) and AB (having non-singular and non-local kernel) fractional operators. From Fig. 3a, as improvement in the estimations of Pr shows that development in the viscosity of liquid declines the difference among thermal boundary layers of the liquid, so the temperature profile declines because of the rises in the estimations of Pr and in the same way, the comparison of two nanofluids is shown in Fig. 3b by considering other parameters constant and changing the fractional parameters α,β. We see that the temperature of the blood-based NF is smaller than the water-based nanofluid, which is due to the physical characteristics of certain nanoparticles.

From Figs. 4a and 4b, we see that the velocity of fluid also decelerates by enhancing the estimation of α,β for a small time but speeds up at a large time. This is also due to the diverse properties of CF (based on exponential function having no singularity) and AB (having non-singular and non-local kernel) fractional operators. The fluid velocity is increased as Gr grows as shown in 5a. The velocity increases because of enhancing the values Gr. The relative impact of the heat buoyant behaviour on the viscous force is investigated using Gr. Such effects happen because of the existence of buoyant forces. An enhancement in the Pr declines the fluid velocity due to development in the fluid viscosity as in 5b Pr is inversely related to thermal diffusivity, resulting in declining heat transmission. The effect of volume fraction (φ) on velocity is illustrated in Fig 6a with the variation in time. The increase in volume fraction enhances the viscous impact of fluid flow which slows down the velocity of the fluid.

In Figs. 7a and 7b, growing the estimation of the magnetic parameter slows down the fluid velocity. Larger estimates of M lead to decreased velocity. Physical applications for such observations are because of the Lorentz force which produces a resistance in the flow. Similarly, the behaviour of the inclination angle of the magnetic field is shown in Fig 7b. The growth in the inclination angle declines the influence of the magnetic field which conveys off the Lorentz force effect, so by growing the estimation of the inclination angle, the fluid velocity again decreases. For $\theta=\pi/2$ (normal magnetic field), the velocity is maximum declined, such observations are because of the Lorentz force which produces resistance in the flow. The Lorentz force has the greatest influence on velocity, decreasing velocity.

The comparison of ordinary and fractional fluid velocity is illustrated in Fig. 8a and 8b for diverse values of fractional parameters. We observe that when the fractional parameter i.e., $\alpha,\beta\to 1$, the fractional fluid velocity almost overlaps with ordinary velocity, which represents the convergence of our obtained numerical solutions of the velocity profile. From the graphical illustration, we see that the results attained by the AB-fractional derivative show more growing behaviour than the CF-fractional derivative. This is also due to the different properties of CF- (based on exponential function having no singularity) and AB (having non-singular and non-local kernel) fractional operators.

The comparison of different nanofluids for velocity field is shown in Fig. 9a. We see that the enhancement in velocity, due to (H_2O-Al_2O_3) and (Blood-Al_2O_3) is more advanced, than (H_2O-TiO_2) and (Blood-TiO_2) based NFs but (H_2O-Al_2O_3) based NF has a higher velocity than (Blood-Al_2O_3) based NF, all this behaviour is due to the physical characteristics of certain nanoparticles. The comparison of numerical methods specifically Grave Stehfest as well as Tzou's is considered in Fig. 9b. The curves of the Stehfests, as well as Tzou's scheme, overlap each other in both cases, which also validates our present results. Furthermore, to make the validity of our attained solutions, the numerical comparison of temperature as well as velocity field through Stehfest and Tzou's with Nusselt number as well as skin friction, are presented in Tables 2-3.

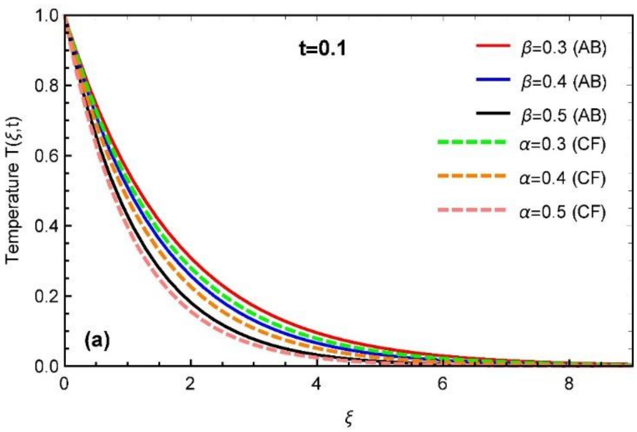

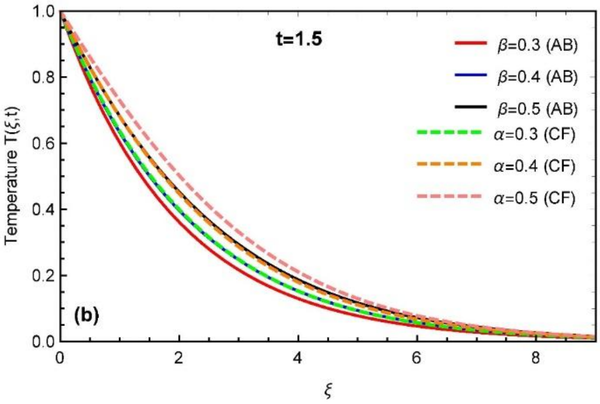

Fig. 2. Plot of temperature field for both fractional models when $Pr = 0.3, \varphi = 0.01$ with (a): $t = 0.1$ and (b): $t = 1.5$

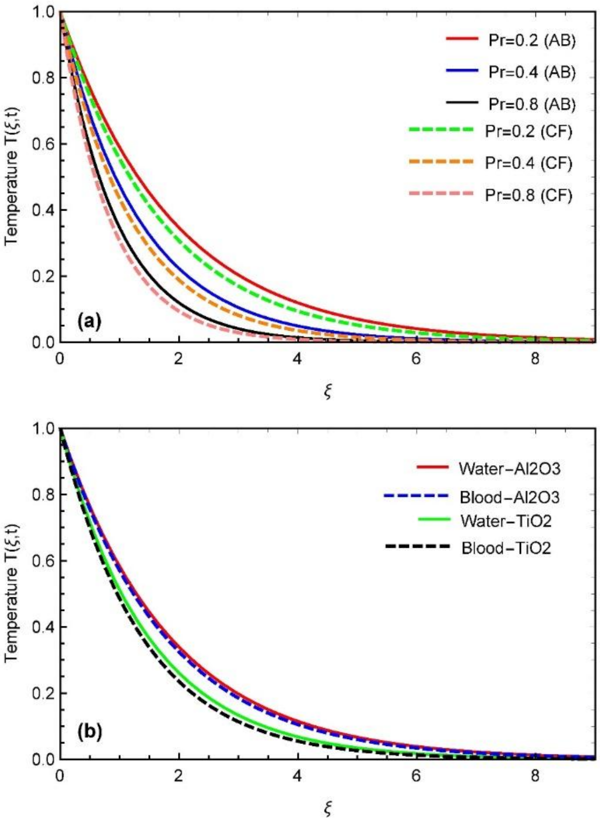

Fig. 3. Temperature field for diverse values of (a): Prandtl number and (b): nanofluid with $\alpha, \beta = 0.5, \varphi = 0.01,$ and $t = 0.1$

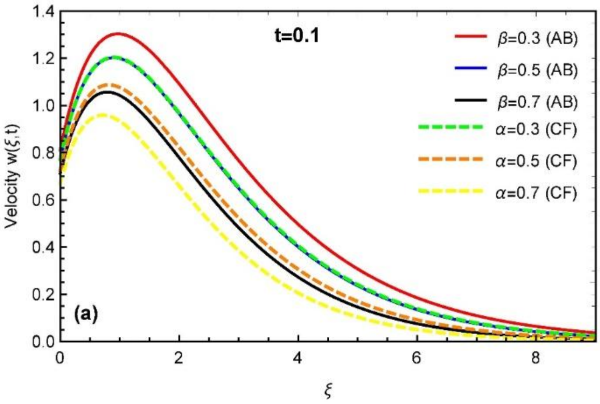

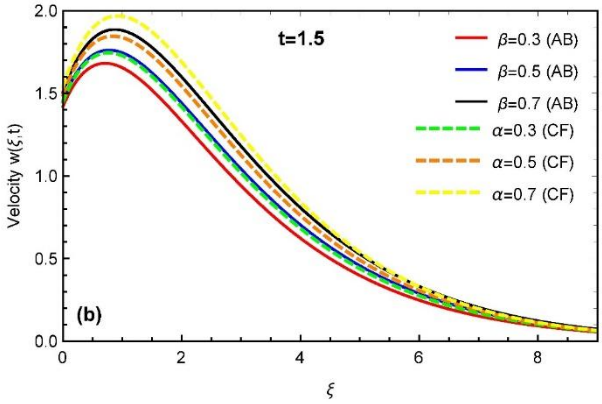

Fig. 4. Effect of (α, β) on velocity for $Pr = 0.3,\ M = 0.5,\ Gr = 4,\ \theta = \frac{\pi}{4}, w = 0.9,\ b = 0.5,\ \delta = \frac{\pi}{4}$ and (a): $t = 0.1$ (b): $t = 1.5$

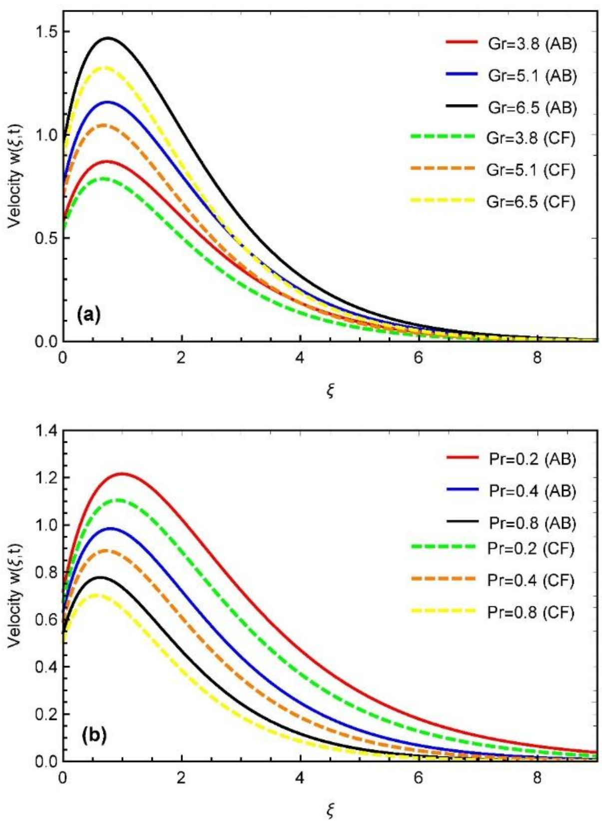

Fig. 5. The effect of (a): Grashof number (b): Pr on velocity when $\alpha, \beta = 0.5,\ M = 0.5,\ \theta = \frac{\pi}{4}, w = 0.9,\ b = 0.5,\ \delta = \frac{\pi}{4},\ t = 0.1$

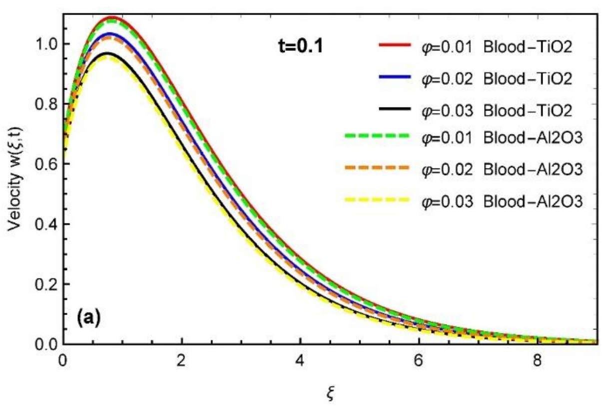

Fig. 6. Effect of volume fraction φ on velocity for $\alpha, \beta = 0.5,\ Pr = 0.3,\ M = 0.5,\ Gr = 4,\ \theta = \frac{\pi}{4}, w = 0.9,\ b = 0.5,\ \delta = \frac{\pi}{4}$

DOI 10.2478/ama-2025-0005

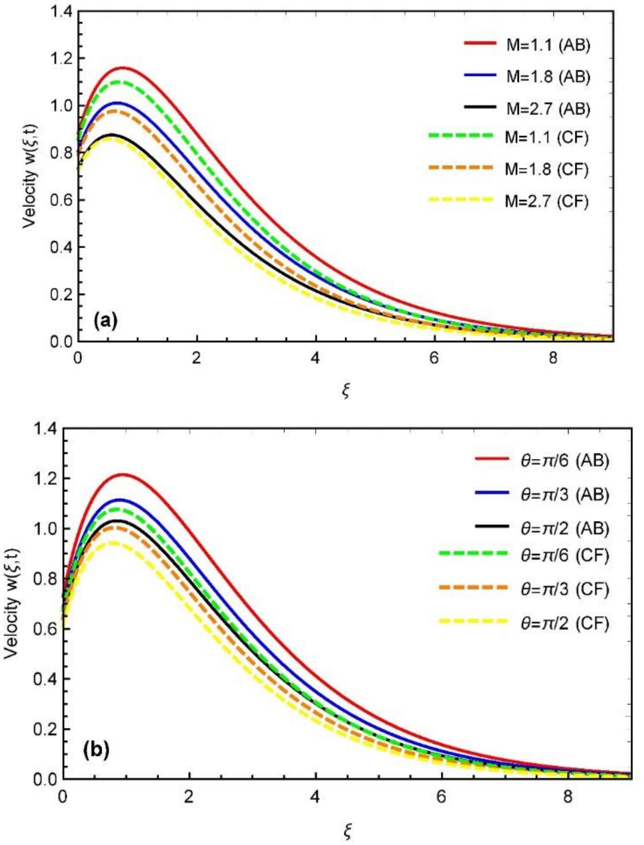

Fig. 7. Variation in (a): magnetic parameter and (b): the inclination of magnetic field for velocity field with $\alpha,\beta = 0.5,\ Pr = 0.3,\ Gr = 4,\ w = 0.9,\ b = 0.5,\ \delta = \frac{\pi}{4},\ t = 0.1$

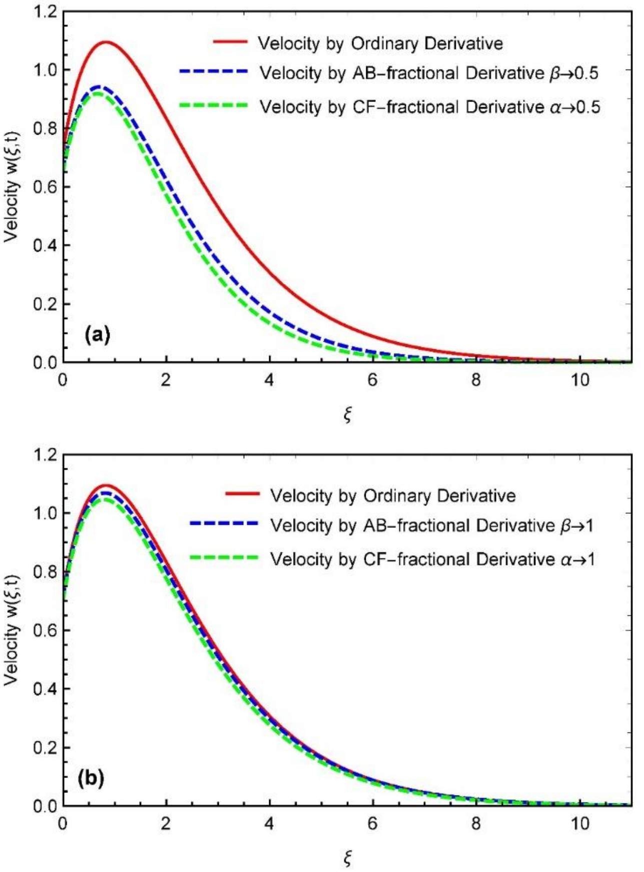

Fig. 8. Comparison of ordinary and fractional velocity when (a): $\alpha,\beta \to 0.5$ and (b): $\alpha,\beta \to 1$

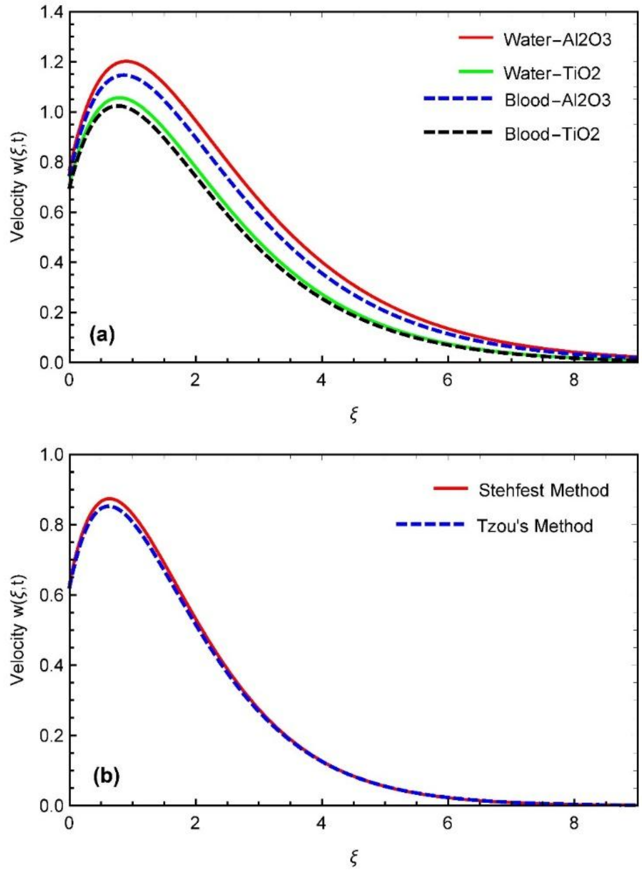

Fig. 9. Comparison of (a): nanofluids and (b): numerical techniques for the velocity field

Tab. 2. A comparison of solutions with two diverse approaches

ξ	Temperature by Stehfest	Temperature by Tzou	Velocity by Stehfest	Velocity by Tzou
0.1	0.9471	0.9471	0.7001	0.6999
0.2	0.8971	0.8971	0.7856	0.7854
0.3	0.8496	0.8496	0.8532	0.8530
0.4	0.8046	0.8046	0.9053	0.9051
0.5	0.7619	0.7619	0.9438	0.9436
0.6	0.7215	0.7215	0.9707	0.9705
0.7	0.6831	0.6831	0.9875	0.9872
0.8	0.6468	0.6468	0.9956	0.9954
0.9	0.6123	0.6123	0.9964	0.9961

DOI 10.2478/ama-2025-0005 acta mechanica et automatica, vol.19 no.1 (2025)

Tab. 3. Numerical analysis of Nusselt number as well as skin friction for CF and AB derivatives

α, β	Nu by CF	Nu by AB	C_f by AB	C_f by CF
0.1	0.5352	0.5309	0.1836	0.1824
0.2	0.5276	0.5204	0.1751	0.1553
0.3	0.5151	0.5053	0.1611	0.1335
0.4	0.4972	0.4842	0.1423	0.1127
0.5	0.4730	0.4558	0.1203	0.0934
0.6	0.4411	0.4193	0.0965	0.0777
0.7	0.4000	0.3761	0.0728	0.0677
0.8	0.3502	0.3326	0.0513	0.0637
0.9	0.2965	0.2996	0.0359	0.0654

7. CONCLUSIONS

We study mixed convection flows over an inclined plate with Al_2O_3 and TiO_2 nanoparticles with water and blood-based fluids along with new definitions of CF (based on exponential function having no singularity) and AB (having non-singular and non-local kernel) fractional operators in several circumstances which is a significant theoretical and practical study for the solution of important problems. A semi-analytical approach for AB and CF-based models is applied by the Laplace transform technique along with Stehfest and Tzou's numerical schemes.

- The temperature shows dual behaviour with different estimations of fractional parameters with diverse estimations (small and large) of the time.
- The temperature displays decaying behaviour for large estimations of the Pr.
- The velocity slows down by growing the estimation of M.
- The velocity profile speeds up as increasing the estimations of Gr and declines for increasing values of volume fraction φ.
- The enhancement in velocity, due to (H_2O-Al_2O_3) and (Blood-Al_2O_3) is more advanced, than (H_2O-TiO_2) and (Blood-TiO_2) based NFs.
- Our obtained solutions through different numerical methods specifically Stehfest and Tzou's are alike.

Consequently, our claimed results offer significant insights into industrial and engineering systems. These findings guide the development of thermal transfer technologies, assisting in the optimization of processes for better efficiency in applications such as cooling mechanisms and power generation. The research advances heat transfer processes, increasing the overall efficiency of industrial systems.

Nomenclature:

Symbol	Quantity	Unit
w	Velocity	(m/s)
t	Time	(s)
T	Temperature	(K)
k_{nf}	Thermal conductivity of nanofluid	(W/mk)
T	Temperature	(K)
T_∞	Ambient temperature	(K)
Gr	Grashof number	$(-)$
M	Dimensionless magnetic parameter	$(-)$
Pr	Prandtl number	$(-)$
q	Laplace transform variable	$(-)$
B_o	Strength of magnetic field	(kg/s^2)
C_p	Specific heat at constant pressure	(J/kgK)
b	Slip parameter	$(-)$
C_f	Skin friction	$(-)$
Nu	Nusselt number	$(-)$

Greek Letters:

μ_{nf}	Dynamic viscosity	(Pa-s)
α, β	Fractional parameters	$(-)$
α_1	Second-grade parameter	$(-)$
β_T	Volumetric coefficient of expansion	$(-)$
ρ_{nf}	Density of nanofluid	(kg/m^3)
θ	The angle of magnetic inclination	$(-)$
δ	The inclination angle of the plate	(mol/m^3)
β_T	Volumetric coefficient of expansion	$(-)$
σ_{nf}	Electrical conductivity of nanofluid	$(-)$
ρ_f	Density of fluid	(kg/m^3)
ρ_s	Density of solid	(kg/m^3)
φ	The volume fraction of nanofluid	$(-)$

Note: This $(-)$ signifies the dimensionless quantity.

Abbreviations:

AB Atangana Baleanu time fractional derivative
NF Nanofluid
CF Caputo-Fabrizio time fractional derivative
MHD Magnetohydrodynamics

DOI 10.2478/ama-2025-0005

REFERENCES

1. Aman S, Abdeljawad T, Al-Mdallal Q. Natural convection flow of a fluid using Atangana and Baleanu fractional model. Advances in Difference Equations. 2020(1):305.
2. Ali FH, Hamzah HK, Egab K, Arıcı M, Shahsavar A. Non-Newtonian nanofluid natural convection in a U-shaped cavity under magnetic field. International Journal of Mechanical Sciences. 2020;186:105887.
3. Tayebi T, Öztop HF, Chamkha AJ. Natural convection and entropy production in hybrid nanofluid filled-annular elliptical cavity with internal heat generation or absorption. Thermal Science and Engineering Progress. 2020;19:100605.
4. Paul A, Deka RK. Unsteady natural convection flow past an infinite cylinder with thermal and mass stratification. International Journal of Engineering Mathematics. 2017(1):8410691.
5. Shaikh TS, Akgül A, Rehman MA, Ahmed N, Iqbal MS, Shahid N, Rafiq M, De la Sen M. A nonlinear structure of a chemical reaction model and numerical modeling with the new aspect of existence and uniqueness. Mathematics. 2022;11(1):37.
6. Amir M, Ali Q, Raza A, Almusawa MY, Hamali W, Ali AH. Computational results of convective heat transfer for fractionalized Brinkman type tri-hybrid nanofluid with ramped temperature and non-local kernel. Ain Shams Engineering Journal. 2024;15(3):102576.
7. Ali Q, Riaz S, Memon IQ, Chandio IA, Amir M, Sarris IE, Abro KA. Investigation of magnetized convection for second-grade nanofluids via Prabhakar differentiation. Nonlinear Engineering. 2023;12(1):20220286.
8. Yasin MW, Ahmed N, Iqbal MS, Rafiq M, Raza A, Akgül A. Reliable numerical analysis for stochastic reaction-diffusion system. Physica Scripta. 2022;98(1):015209.
9. Awan AU, Ali Q, Riaz S, Shah NA, Chung JD. A thermal optimization throughan innovative mechanism of free convection flow of Jeffrey fluid using non-local kernel. Case Studies in Thermal Engineering. 2021;24:100851.
10. Riaz S, Sattar M, Abro KA, Ali Q. Thermo-dynamical investigation of constitutive equation for rate type fluid: a semi-analytical approach. International Journal of Modelling and Simulation. 2023;43(3):123-34.
11. Ali Q, Riaz S, Awan AU, Abro KA. A mathematical model for thermography on viscous fluid based on damped thermal flux. Zeitschrift für Naturforschung A. 2021;76(3):285-94.
12. Ajeel RK, Salim WI, Hasnan K. Design characteristics of symmetrical semicircle-corrugated channel on heat transfer enhancement with nanofluid. International Journal of Mechanical Sciences. 2019;151:236-50.
13. Abro KA, Atangana A, Gomez-Aguilar JF. An analytic study of bioheat transfer Pennes model via modern non-integers differential techniques. The European Physical Journal Plus. 2021;136:1-1.
14. Abro KA, Abdon A. A computational technique for thermal analysis in coaxial cylinder of one-dimensional flow of fractional Oldroyd-B nanofluid. International Journal of Ambient Energy. 2022;43(1): 5357-65.
15. Ganvir RB, Walke PV, Kriplani VM. Heat transfer characteristics in nanofluid—A review. Renewable and sustainable energy reviews. 2017;75:451-60.
16. Aman S, Khan I, Ismail Z, Salleh MZ. Applications of fractional derivatives to nanofluids: exact and numerical solutions. Mathematical Modelling of Natural Phenomena. 2018;13(1):2.
17. Hussanan A, Trung NT. Heat transfer analysis of sodium carboxymethyl cellulose based nanofluid with titania nanoparticles. Journal of Advanced Research in Fluid Mechanics and Thermal Sciences. 2019;56(2):248-56.
18. Farhana K, Kadirgama K, Noor MM, Rahman MM, Ramasamy D, Mahamude AS. CFD modelling of different properties of nanofluids in header and riser tube of flat plate solar collector. InIOP Conference Series: Materials Science and Engineering 2019, 469: 012041.
19. Jamshed W, Aziz A. A comparative entropy based analysis of Cu and Fe3O4/methanol Powell-Eyring nanofluid in solar thermal collectors subjected to thermal radiation, variable thermal conductivity and impact of different nanoparticles shape. Results in physics. 2018; 9:195-205.
20. Jamshed W, Goodarzi M, Prakash M, Nisar KS, Zakarya M, Abdel-Aty AH. Evaluating the unsteady Casson nanofluid over a stretching sheet with solar thermal radiation: An optimal case study. Case Studies in Thermal Engineering. 2021; 26:101160.
21. Jamshed W, Nisar KS, Gowda RP, Kumar RN, Prasannakumara BC. Radiative heat transfer of second grade nanofluid flow past a porous flat surface: a single-phase mathematical model. Physica Scripta. 2021;96(6):064006.
22. Jamshed W, Nisar KS, Ibrahim RW, Mukhtar T, Vijayakumar V, Ahmad F. Computational frame work of Cattaneo-Christov heat flux effects on Engine Oil based Williamson hybrid nanofluids: A thermal case study. Case Studies in Thermal Engineering. 2021; 26:101179.
23. Jamshed W, Devi SU, Nisar KS. Single phase based study of Ag-Cu/EO Williamson hybrid nanofluid flow over a stretching surface with shape factor. Physica Scripta. 2021;96(6):065202.
24. Jamshed W, Eid MR, Rehman S, Mohamed Isa SS, Abd-Elmonem A, Alanzi AM, Farooq S. Numerical heat and solutal transfer simulation of fluid flowing via absorptive shrinkable sheet with Ohmic heat resistance. Numerical Heat Transfer, Part A: Applications. 2024;85(10):1552-68.
25. Aziz A, Jamshed W, Aziz T, Bahaidarah HM, Ur Rehman K. Entropy analysis of Powell–Eyring hybrid nanofluid including effect of linear thermal radiation and viscous dissipation. Journal of Thermal Analysis and Calorimetry. 2021;143(2):1331-43.
26. Sajid T, Gari AA, Jamshed W, Eid MR, Islam N, Irshad K, Altamirano GC, El Din SM. Case study of autocatalysis reactions on tetra hybrid binary nanofluid flow via Riga wedge: Biofuel thermal application. Case Studies in Thermal Engineering. 2023; 47:103058.
27. Kai Y, Ali K, Ahmad S, Ahmad S, Jamshed W, Raizah Z, El Din SM. A case study of different magnetic strength fields and thermal energy effects in vortex generation of Ag-TiO2 hybrid nanofluid flow. Case Studies in Thermal Engineering. 2023; 47:103115.
28. Hanif H, Jamshed W, Eid MR, Ibrahim RW, Shafie S, Raezah AA, El Din SM. Numerical Crank-Nicolson methodology analysis for hybridity aluminium alloy nanofluid flowing based-water via stretchable horizontal plate with thermal resistive effect. Case Studies in Thermal Engineering. 2023; 42:102707.
29. Kai Y, Ahmad S, Takana H, Ali K, Jamshed W, Eid MR, Abd-Elmonem A, El Din SM. Thermal case study and generated vortices by dipole magnetic field in hybridized nanofluid flowing: Alternating direction implicit solution. Results in Physics. 2023; 49:106464.
30. Ullah I, Ali F, Isa SM, Murtaza S, Jamshed W, Eid MR, Amjad A, Guedri K, Khalifa HA, El Din SM. Electro-magnetic radiative flowing of Williamson-dusty nanofluid along elongating sheet: Nanotechnology application. Arabian Journal of Chemistry. 2023;16(5):104698.
31. Zhang X, Yang D, Katbar NM, Jamshed W, Ullah I, Eid MR, Raizah Z, Ibrahim RW, Khalifa HA, El Din SM. Entropy and thermal case description of monophase magneto nanofluid with thermal jump and Ohmic heating employing finite element methodology. Case Studies in Thermal Engineering. 2023;45:102919.
32. Podlubny I. Fractional differential equations: an introduction to fractional derivatives, fractional differential equations, to methods of their solution and some of their applications. elsevier; 1998, 198:1-340.
33. Baleanu D, Fernandez A. On fractional operators and their classifications. Mathematics. 2019;7(9):830.
34. Wang BO, Tahir M, Imran M, Javaid M, Jung CY. Semi analytical solutions for fractional Oldroyd-B fluid through rotating annulus. IEEE Access. 2019; 7:72482-91.
35. Ullah Z, Abbas A, El-Zahar ER, Seddek LF, Akgul A, Hassan AM. Significance of thermal density and viscous dissipation on heat and mass transfer of chemically reactive nanofluid flow along stretching sheet under magnetic field. Results in Engineering. 2023; 20:101413.
36. Ahmed N, Baber MZ, Iqbal MS, Annum A, Ali SM, Ali M, Akgül A, El Din SM. Analytical study of reaction diffusion Lengyel-Epstein system by generalized Riccati equation mapping method. Scientific Reports.

2023;13(1):20033.
37. Caputo M, Fabrizio M. A new definition of fractional derivative without singular kernel. Progress in Fractional Differentiation & Applications. 2015;1(2):73-85.
38. Qayyum M, Afzal S, Saeed ST, Akgül A, Riaz MB. Unsteady hybrid nanofluid (Cu-UO2/blood) with chemical reaction and non-linear thermal radiation through convective boundaries: An application to bio-medicine. Heliyon. 2023;9(6):e16578.
39. Ahmad B, Ahmad MO, Farman M, Akgül A, Riaz MB. A significance of multi slip condition for inclined MHD nano-fluid flow with non linear thermal radiations, Dufuor and Sorrot, and chemically reactive bio-convection effect. South African Journal of Chemical Engineering. 2023;43:135-45.
40. Riaz S, Sattar M, Abro KA, Ali Q. Thermo-dynamical investigation of constitutive equation for rate type fluid: a semi-analytical approach. International Journal of Modelling and Simulation. 2023;43(3):123-34.
41. Atangana A, Baleanu D. New fractional derivatives with nonlocal and non-singular kernel: theory and application to heat transfer model. arXiv preprint arXiv:1602.03408. 2016.
42. Riaz MB, Iftikhar N. A comparative study of heat transfer analysis of MHD Maxwell fluid in view of local and nonlocal differential operators. Chaos, Solitons & Fractals. 2020;132:109556.
43. Atangana A. On the new fractional derivative and application to non-linear Fisher's reaction–diffusion equation. Applied Mathematics and computation. 2016;273:948-56.
44. Riaz S, Ali Q, Khanam Z, Rezazadeh H, Esfandian H. Modeling and computation of nanofluid for thermo-dynamical analysis between vertical plates. Proceedings of the Institution of Mechanical Engineers, Part E: Journal of Process Mechanical Engineering. 2023;237(5):1750-60.
45. Riaz S, Amir M, Memon IQ, Ali Q, Abro KA. A comparative study for solidification of nanoparticles suspended in nanofluids through non-local kernel approach. Arabian Journal for Science and Engineering. 2023;48(9):11645-63.
46. Riaz S, Ali S, Ali Q, Khan SU, Amir M. Fractional simulations for mixed convection flow of hybrid nanofluids due to inclined channel with chemical reaction and external heat source features. Waves in Random and Complex Media. 2023;1-9.
47. Ali Q, Yassen MF, Asiri SA, Pasha AA, Abro KA. Role of viscoelasticity on thermoelectromechanical system subjected to annular regions of cylinders in the existence of a uniform inclined magnetic field. The European Physical Journal Plus. 2022;137(7):1-0.
48. Stehfest H. Algorithm 368: Numerical inversion of Laplace transforms [D5]. Communications of the ACM. 1970;13(1):47-9.
49. Tzou DY. Macro-to microscale heat transfer: the lagging behavior. John Wiley & Sons; 2014.

Dr. Kashif Ali Abro is thankful to Mehran University of Engineering and Technology, Jamshoro, Pakistan, for the generous support and facilities of this research work.

Qasim Ali: https://orcid.org/0000-0003-4118-4515

Rajai S. Alassar: https://orcid.org/0000-0003-3084-7782

Irfan. A. Abro: https://orcid.org/0000-0001-9350-0407

Kashif. A. Abro: https://orcid.org/0000-0003-0867-642X